

## Pion-Induced Radiative Corrections to Neutron $\beta$ Decay

Vincenzo Cirigliano<sup>1,2,\*</sup> Jordy de Vries<sup>3,4,†</sup> Leendert Hayen<sup>5,6,‡</sup>  
 Emanuele Mereghetti<sup>1,§</sup> and André Walker-Loud<sup>7,||</sup>

<sup>1</sup>*Los Alamos National Laboratory, Theoretical Division T-2, Los Alamos, New Mexico 87545, USA*

<sup>2</sup>*Institute for Nuclear Theory, University of Washington, Seattle, Washington 98195-1550, USA*

<sup>3</sup>*Institute for Theoretical Physics Amsterdam and Delta Institute for Theoretical Physics, University of Amsterdam, Science Park 904, 1098 XH Amsterdam, Netherlands*

<sup>4</sup>*Nikhef, Theory Group, Science Park 105, 1098 XG Amsterdam, Netherlands*

<sup>5</sup>*Department of Physics, North Carolina State University, Raleigh, North Carolina 27695, USA*

<sup>6</sup>*Triangle Universities Nuclear Laboratory, Durham, North Carolina 27708, USA*

<sup>7</sup>*Nuclear Science Division, Lawrence Berkeley National Laboratory, Berkeley, California 94720, USA*

 (Received 4 March 2022; revised 10 June 2022; accepted 3 August 2022; published 12 September 2022)

We compute the electromagnetic corrections to neutron  $\beta$  decay using a low-energy hadronic effective field theory. We identify new radiative corrections arising from virtual pions that were missed in previous studies. The largest correction is a percent-level shift in the axial charge of the nucleon proportional to the electromagnetic part of the pion-mass splitting. Smaller corrections, comparable to anticipated experimental precision, impact the  $\beta$ - $\nu$  angular correlations and the  $\beta$  asymmetry. We comment on implications of our results for the comparison of the experimentally measured nucleon axial charge with first-principles computations using lattice QCD and on the potential of  $\beta$  decay experiments to constrain beyond-the-standard-model interactions.

DOI: [10.1103/PhysRevLett.129.121801](https://doi.org/10.1103/PhysRevLett.129.121801)

*Introduction.*—High-precision measurements of low-energy processes, such as  $\beta$  decays of mesons, neutron, and nuclei, probe the existence of new physics at very high energy scales through quantum fluctuations. Recent developments in the study of  $\beta$  decay rates at the subpercent level [1–5] have led to a 3–5 $\sigma$  tension with the standard model (SM) interpretation in terms of the unitary Cabibbo-Kobayashi-Maskawa (CKM) quark mixing matrix [5,6]. Further, global analyses of  $\beta$  decay observables [7,8] have highlighted additional avenues for  $\beta$  decays to probe physics beyond the standard model (BSM) at the multi-TeV scale, such as the comparison of the experimentally extracted weak axial charge  $g_A$  with precise lattice quantum chromodynamics (QCD) calculations [9–11]. This test is a unique and sensitive probe of BSM right-handed charged currents.

Given the expected improvements in experimental precision in the next few years [12–14], a necessary condition to use neutron decay as probe of BSM physics is to have high-precision calculations *within* the SM, including subpercent level recoil and radiative corrections with controlled uncertainties. These prospects have spurred new theoretical activity, which has focused first on radiative corrections to the strength of the Fermi transition (vector coupling) [1–4], and more recently on the corrections to the Gamow-Teller (axial) coupling [15,16]. These recent studies are all rooted in the current algebra approach developed in the 1960s and

1970s [17,18], combined with the novel use of dispersive techniques.

In principle, lattice QCD can be used to compute the full standard model  $n \rightarrow pe\bar{\nu}$  decay amplitude including radiative QED corrections, similar to the determination of the leptonic pion decay rate [19,20]. However, it will be some years before these calculations reach sufficient precision. Currently, lattice QCD calculations are carried out in the isospin limit. The global average determination of  $g_A$  carries a 2.2% uncertainty [21] with one result achieving a 0.74% uncertainty [11,22]. The Particle Data Group (PDG) average value, on the other hand, has a 0.1% uncertainty [6] with the most precise experiment having a 0.035% uncertainty [23].

In this Letter, we present a systematic effective field theory (EFT) study of radiative corrections to the neutron decay differential decay rate given by [9,24–26]

$$\frac{d\Gamma}{dE_e d\Omega_e d\Omega_\nu} = \frac{(G_F V_{ud})^2}{(2\pi)^5} (1 + 3\lambda^2) w(E_e) \times \left[ 1 + \bar{a}(\lambda) \frac{\vec{p}_e \cdot \vec{p}_\nu}{E_e E_\nu} + \bar{A}(\lambda) \frac{\vec{\sigma}_n \cdot \vec{p}_e}{E_e} + \dots \right], \quad (1)$$

where  $G_F$  is the Fermi constant,  $V_{ud}$  is the up-down CKM matrix element,  $w(E_e)$  describes the electron spectrum,  $\vec{\sigma}_n$  denotes the neutron polarization, and  $\lambda \equiv g_A/g_V$  is the ratio of the weak vector (axial) couplings defined in Eq. (2)

below, which in the absence of radiative corrections reduces to the nucleon isovector vector (axial) charges. Correlation coefficients such as  $\bar{a}(\lambda)$  and  $\bar{A}(\lambda)$  can be precisely measured and allow for an experimental determination of  $\lambda$ . In Eq. (1) we kept terms of relevance for the present discussion and refer to Supplemental Material [27] for the full expressions.

In the EFT framework we compute new structure-dependent electromagnetic corrections originating at the pion mass scale, including effects up to  $\mathcal{O}(\alpha)$ ,  $\mathcal{O}(am_\pi/m_N)$ , and  $\mathcal{O}(am_e/m_\pi)$ , with  $\alpha = e^2/4\pi$  the fine-structure constant,  $m_e$  the electron mass, and  $m_\pi(m_N)$  the pion (nucleon) mass. By doing so we uncover new *percent-level* electromagnetic corrections to the axial coupling  $g_A$ , which were missed both in the only other neutron  $\beta$  decay EFT analysis [25] and recent dispersive treatments [15,16]. These corrections affect the comparison between the present lattice-QCD results for the nucleon axial charge  $g_A^{\text{QCD}}$  and the experimentally determined  $\lambda$  [see Eq. (11) and subsequent discussion]. In addition, our new corrections imply measurable changes in the decay correlations in Eq. (1) [see Eq. (15)].

*Neutron decay from the standard model.*—The energy release in neutron decay is roughly the mass splitting of the neutron and proton, i.e.,  $q_{\text{ext}} \sim m_n - m_p \sim 1$  MeV, which is significantly smaller than the nucleon mass. The energy scale of nucleon structure corrections, on the other hand, is related to the pion mass, so that  $m_N \gg m_\pi \gg m_n - m_p$ . As a consequence, corrections to neutron  $\beta$  decay can be parametrized in terms of two small parameters: (i)  $\epsilon_{\text{recoil}} = q_{\text{ext}}/m_N \sim 0.1\%$  which characterizes small kinetic corrections; (ii)  $\epsilon_\pi = q_{\text{ext}}/m_\pi \sim 1\%$ , which characterizes nucleon structure corrections dominated by pion contributions. At these relatively low energies, the decay amplitude can be described by a nonrelativistic Lagrangian density (see also Refs. [25,32])

$$\begin{aligned} \mathcal{L}_\# = & -\sqrt{2}G_F V_{ud} \left\{ \bar{e} \gamma_\mu P_L \nu_e \left[ \bar{N} (g_V v^\mu - 2g_A S^\mu) \tau^+ N \right. \right. \\ & + \left. \frac{i}{2m_N} \bar{N} (v^\mu v^\nu - g^{\mu\nu} - 2g_A v^\mu S^\nu) (\bar{\partial} - \vec{\partial})_\nu \tau^+ N \right] \\ & + \frac{ic_T m_e}{m_N} \bar{N} (S^\mu v^\nu - S^\nu v^\mu) \tau^+ N (\bar{e} \sigma_{\mu\nu} P_L \nu) \\ & \left. + \frac{i\mu_{\text{weak}}}{m_N} \bar{N} [S^\mu, S^\nu] \tau^+ N \partial_\nu (\bar{e} \gamma_\mu P_L \nu) \right\} + \dots, \quad (2) \end{aligned}$$

where pions have been integrated out (hence subscript  $\#$ ), and the ellipsis denote terms not affected by our analysis. In this expression,  $N^T = (p, n)$  is an isodoublet of nucleons, while  $v_\mu$  and  $S_\mu$  represent the velocity and spin of the nucleon, respectively. The effective vector and axial-vector couplings,  $g_V$  and  $g_A$ , reduce to the isovector nucleon vector and axial charges if one ignores radiative corrections, while

$\mu_{\text{weak}}$  and  $c_T$  are the weak magnetic moment and an effective tensor coupling, respectively. Equation (2) can be used to compute the differential neutron decay rate and the parameters can then be fitted to data.

There are a number of shortcomings to this approach. First, by utilizing measured values of  $V_{ud}g_V$ ,  $g_A/g_V$ ,  $\mu_{\text{weak}}$ , and  $c_T$ , we neither extract fundamental SM parameters nor distinguish SM from BSM contributions to these low-energy constants (LECs). Second, it is not possible to disentangle, for example, how much of  $g_A$  arises from isospin symmetric QCD versus electromagnetic contributions. Therefore, it is desirable to utilize an EFT which encodes the corrections as functions of the SM parameters, such as the quark masses and the electromagnetic couplings. This is known as chiral perturbation theory ( $\chi$ PT) [33,34], or specifically for baryons, heavy baryon  $\chi$ PT (HB $\chi$ PT) [35]. The cost of such a description is the introduction of new scales,  $m_\pi$  and  $\Lambda_\chi = 4\pi F_\pi \sim 1$  GeV with  $F_\pi \simeq 92.4$  MeV, which form another expansion parameter,  $\epsilon_\chi = m_\pi/\Lambda_\chi$ , and new operators with potentially undetermined LECs.

In light of the above discussion, radiative corrections to neutron decay can be organized in a double expansion in  $\alpha\epsilon_\chi^n\epsilon_\pi^m$ . First, we integrate out the pions and match the  $\chi$ PT amplitude to the  $\#$ EFT amplitude, thus determining the quark mass and electromagnetic corrections to effective couplings such as  $g_A$ . Then, the neutron decay amplitude can be computed with  $\#$ EFT (with dynamical photons and leptons) while retaining explicit sensitivity to the parameters of the standard model. In our analysis of the decay amplitude we retain terms of  $\mathcal{O}(G_F\epsilon_{\text{recoil}})$ , known in the literature,  $\mathcal{O}(G_F\alpha)$ , where we uncover previously overlooked effects, and terms of  $\mathcal{O}(G_F\alpha\epsilon_\chi)$  and  $\mathcal{O}(G_F\alpha\epsilon_\pi)$ , never before considered in the literature.

*$\chi$ PT setup for neutron decay.*—To study radiative corrections to weak semileptonic transitions, we adopt the HB $\chi$ PT framework [35] with dynamical photons [36–38] and leptons, in analogy with the meson sector [39]. This EFT provides a necessary intermediate step in the analysis of neutron decay, before integrating out pions, and is the starting point for the study of related processes such as muon capture, low-energy neutrino-nucleus scattering, and nuclear  $\beta$  decays, which of course require a nontrivial generalization to multi-nucleon effects.

In  $\chi$ PT with dynamical photons and leptons, semileptonic amplitudes are expanded in the Fermi constant  $G_F$  (to first order), the electromagnetic fine structure constant  $\alpha$ , and  $\epsilon_\chi$ , while keeping all orders in  $q_{\text{ext}}/m_\pi$ , according to Weinberg's power counting [40–42]. Following standard practice, derivatives ( $\partial \sim p$ ) and the electroweak couplings  $e$ ,  $G_F$  are assigned chiral dimension one, while the light quark mass is assigned chiral dimension two ( $m_\pi^2 \sim p^2$ ).

The leading amplitude  $\mathcal{A}^{G_F p^0}$  arises from one insertion of the lowest order Lagrangian  $\mathcal{L}_{\pi N}^p$

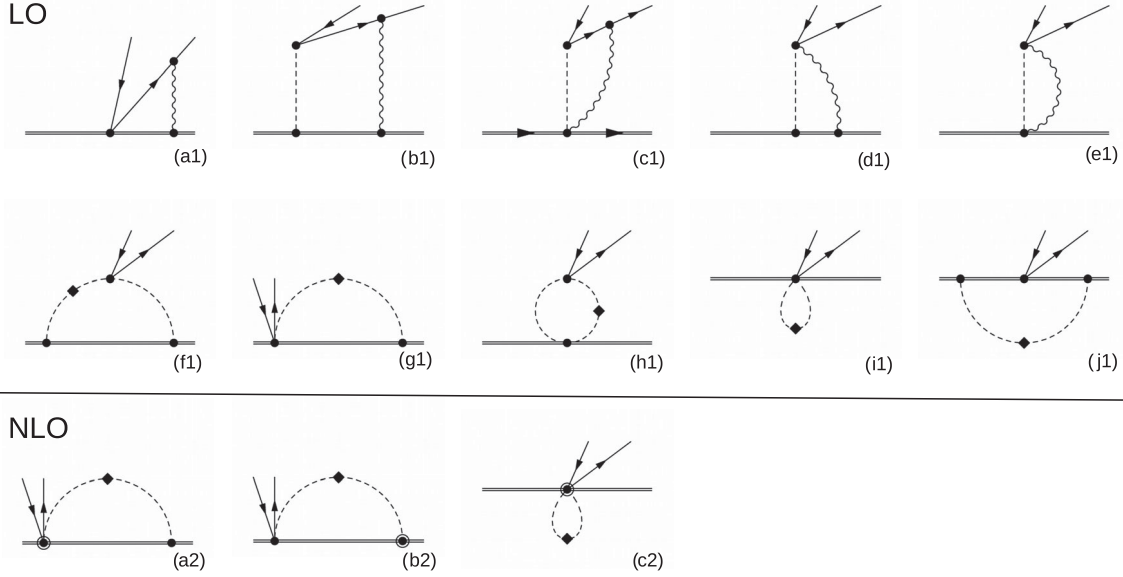


FIG. 1. Diagrams contributing to the matching between  $\chi$ PT and  $\not{n}$ EFT at  $\mathcal{O}(G_F\alpha)$  (upper panel) and  $\mathcal{O}(G_F\alpha\epsilon_\chi)$  (lower panel). Single, double, wavy, and dashed lines denote, respectively, leptons, nucleons, photons, and pions. Dots refer to interactions from the lowest-order chiral Lagrangians, while diamonds represent insertions of  $\mathcal{L}_\pi^{e^2 p^0}$ . Circled dots denote interactions from the NLO pion-nucleon Lagrangian.

$$\mathcal{L}_{\pi N}^p \supset -\sqrt{2}G_F V_{ud}\bar{N}(v^\mu - 2g_A^{(0)}S^\mu)\tau^+ N\bar{e}\gamma_\mu P_L\nu_e, \quad (3)$$

where  $g_A^{(0)}$  denotes the nucleon axial charge in the chiral limit and in absence of electromagnetic effects.

To capture electromagnetic corrections to  $\mathcal{O}(G_F\alpha)$ ,  $\mathcal{O}(G_F\alpha\epsilon_\chi)$ , and  $\mathcal{O}(G_F\alpha\epsilon_\pi)$ , we need to compute the neutron decay amplitude to chiral dimension three ( $\mathcal{A}^{e^2 G_F p^0}$ ) and four ( $\mathcal{A}^{e^2 G_F p}$ ). The former arises from one-loop diagrams involving virtual nucleons, pions, photons, and charged leptons, with vertices from  $\mathcal{L}_{\pi N}^p$  and from the leading order electromagnetic mesonic Lagrangian  $\mathcal{L}_\pi^{e^2 p^0}$  (see Fig. 1, upper panel). Here, an important role is played by insertions of

$$\mathcal{L}_\pi^{e^2 p^0} = 2e^2 F_\pi^2 Z_\pi \pi^+ \pi^- + \mathcal{O}(\pi^4), \quad (4)$$

with the LEC  $Z_\pi$  fixed by the relation  $m_{\pi^\pm}^2 - m_{\pi^0}^2 = 2e^2 F_\pi^2 Z_\pi$ , up to higher-order corrections. Additional contributions arise from tree-level graphs with one insertion of higher-order Lagrangians. Finally, the  $\mathcal{A}^{e^2 G_F p}$  amplitude is a combination of one-loop diagrams with one vertex from higher order Lagrangians  $\mathcal{L}_{\pi N}^{p^2}$  or  $\mathcal{L}_{\pi N}^{e^2 p^0}$  (see Fig. 1, lower panel). All relevant effective Lagrangians are presented in Supplemental Material [27], including a new one needed to absorb divergences from loops involving virtual baryons, photons, and leptons.

*Matching at  $\mathcal{O}(\alpha)$  and  $\mathcal{O}(\alpha\epsilon_\chi)$ .*—The diagrams contributing to the matching between  $\chi$ PT and  $\not{n}$ EFT at  $\mathcal{O}(\epsilon_\chi^0)$  and  $\mathcal{O}(\epsilon_\chi)$  are shown in Fig. 1. They imply for the leading vector and axial operators

$$g_{V/A} = g_{V/A}^{(0)} \left[ 1 + \sum_{n=2}^{\infty} \Delta_{V/A,\chi}^{(n)} + \frac{\alpha}{2\pi} \sum_{n=0}^{\infty} \Delta_{V/A,\text{em}}^{(n)} + \left( \frac{m_u - m_d}{\Lambda_\chi} \right)^{n_{V/A}} \sum_{n=0}^{\infty} \Delta_{V/A,\delta m}^{(n)} \right], \quad (5)$$

where  $g_V^{(0)} = 1$ ,  $\Delta_{\chi,\text{em},\delta m}^{(n)} \sim \mathcal{O}(\epsilon_\chi^n)$ , and  $n_A = 1$ ,  $n_V = 2$  [43,44]. Explicit calculation gives  $\Delta_{A,\delta m}^{(0),(1)} = 0$  and  $\Delta_{V,\delta m}^{(0)} = 0$  to the order we work. A nonzero  $\Delta_{V,\delta m}^{(0)}$ , such as estimated in Ref. [45], arises to higher order in the EFT framework. Concerning the chiral corrections in the isospin limit,  $\Delta_{V,\chi}^{(n)}$  vanish due to conservation of the vector current, while  $\Delta_{A,\chi}^{(n)}$  have been calculated up to  $n = 4$  in Refs. [46–48], and can for our purposes be absorbed into a definition of  $g_A$  in the isospin limit, which we denote by  $g_A^{\text{QCD}}$ .

To  $\mathcal{O}(\alpha\epsilon_\chi^0)$  we consider the diagrams in Fig. 1, upper panel. Diagram (a1) appears in the same form in both EFTs, and thus does not contribute to the matching. An explicit calculation shows that the  $\mathcal{O}(\epsilon_\pi^0)$  term of diagrams (b1) and (d1) and (c1) and (e1) cancels, leaving  $\mathcal{O}(\epsilon_\pi)$  corrections discussed below. Diagrams (g1) and (j1) vanish exactly at  $\mathcal{O}(\epsilon_\chi^0)$ , while (f1), (h1), and (i1) contribute to the vector operator only to be canceled by corrections to the nucleon wave function renormalization (WFR) at zero momentum transfer ( $q = 0$ ). As a consequence,  $g_V$  does not receive loop corrections in the matching between  $\chi$ PT and  $\not{n}$ EFT, instead picking up contributions only from local operators of  $\mathcal{O}(e^2 p)$  so that

$\Delta_{V,\text{em}}^{(0)} = \hat{C}_V$ . By contrast, the axial operator is modified through diagram (i1), the WFR, and local operators of  $\mathcal{O}(e^2 p)$ , leading to

$$\Delta_{A,\text{em}}^{(0)} = Z_\pi \left[ \frac{1 + 3g_A^{(0)2}}{2} \left( \log \frac{\mu^2}{m_\pi^2} - 1 \right) - g_A^{(0)2} \right] + \hat{C}_A(\mu). \quad (6)$$

Here,  $\mu$  denotes the renormalization scale that appears in the dimensionally regularized chiral loops. We provide in Supplemental Material [27] the explicit dependence of  $\hat{C}_{V,A}$  on the LECs of  $\mathcal{O}(e^2 p)$ . Here, we note that as written,  $\hat{C}_{V,A}$  contain information about short-distance physics and in particular large logarithms connecting the weak scale and the hadronic scale [18,49–51] and finite terms that have been calculated via dispersive methods [1–4].

A similar analysis applies to the next-to-leading order (NLO) amplitude, for which we report a few representative diagrams in the lower panel of Fig. 1. At  $q = 0$ , all diagrams contributing to the vector operator are canceled by the WFR, resulting in  $\Delta_{V,\text{em}}^{(1)} = 0$ . The correction to  $g_A$  is

$$\Delta_{A,\text{em}}^{(1)} = Z_\pi 4\pi m_\pi \left[ c_4 - c_3 + \frac{3}{8m_N} + \frac{9}{16m_N} g_A^{(0)2} \right], \quad (7)$$

dominated by the NLO  $\pi N$  LECs  $c_{3,4}$  via topology (a2).

*Matching at  $\mathcal{O}(\alpha\epsilon_\pi)$ .*—Through our final matching step, we identify additional isospin breaking terms to the LECs of the pion-less Lagrangian. Specifically, the pion loops with the vector current coupling to two pions [topology (f1)] induce an isospin-breaking correction to the weak magnetism term. In terms of the physical nucleon magnetic moments,  $\mu_{n/p}$ , we find

$$\delta\mu_{\text{weak}} = \mu_{\text{weak}} - (\mu_p - \mu_n) = -\frac{\alpha Z_\pi g_A^2 m_N \pi}{2\pi m_\pi}. \quad (8)$$

Finally, the pion- $\gamma$  box (b1) induces the tensor coupling

$$c_T = \frac{\alpha g_A m_N \pi}{2\pi 3m_\pi}. \quad (9)$$

*Connection to previous literature.*—Recent approaches using current algebra and dispersion techniques [15,16] evaluated axial contributions as originating from vertex corrections, in which the virtual photon is emitted and absorbed by the hadronic line, and  $\gamma W$  box, in which the virtual photon is exchanged between the hadronic and electron lines. The latter was found to be largely consistent with the vector contribution using experimental data of the polarized Bjorken sum rule [15] and additional nucleon scattering data [16]. The vertex corrections, on the other hand, have only been calculated in limiting scenarios. Following the notation of Ref. [15], the contribution depends on a three-point function

$$\mathcal{D}_\gamma = \int \frac{d^4 k}{k^2} \int d^4 y e^{i\bar{q}y} \int d^4 x e^{ikx} \times \langle p_f | T \{ \partial_\mu J_W^\mu(y) J_\gamma^\lambda(x) J_\lambda^\gamma(0) \} | p_i \rangle, \quad (10)$$

where  $\gamma(W)$  denotes electromagnetic (weak) currents, and  $T\{\dots\}$  the time-ordered product. At large momentum, this expression was evaluated with the operator product expansion, finding  $\mathcal{D}_\gamma^{\text{OPE}} = 0$  in the isospin limit. For more general momentum scales, the integral was approximated by retaining only the on-shell nucleon states with their elastic form factors, concluding  $\mathcal{D}_\gamma \approx 0$  [15]. Our Letter goes beyond this elastic approximation by capturing through EFT, the leading pion contributions to  $\mathcal{D}_\gamma$ .

*Numerical impact.*—We now estimate the numerical impact of the various corrections starting with our main new finding, i.e., the electromagnetic shift to  $\lambda = g_A/g_V$ . Including BSM contributions, the relation between the experimentally extracted  $\lambda$  and the (isosymmetric) QCD axial charge is given by [9]

$$\lambda = g_A^{\text{QCD}} [1 + \delta_{\text{RC}}^{(\lambda)} - 2\text{Re}(\epsilon_R)], \quad (11)$$

where  $\epsilon_R \sim (246 \text{ GeV} / \Lambda_{\text{BSM}})^2$  is a BSM right-handed current contribution appearing at an energy scale  $\Lambda_{\text{BSM}}$  [9,10]. To the order we are working the radiative correction is

$$\delta_{\text{RC}}^{(\lambda)} = \frac{\alpha}{2\pi} (\Delta_{A,\text{em}}^{(0)} + \Delta_{A,\text{em}}^{(1)} - \Delta_{V,\text{em}}^{(0)}). \quad (12)$$

For the numerical evaluation of the loop contributions to  $\Delta_{A,\text{em}}^{(0),(1)}$  we use  $Z_\pi = 0.81$  (obtained from the physical pion mass difference and  $F_\pi = 92.4$  MeV) and the average nucleon mass  $m_N = 938.9$  MeV. In the loops we set  $g_A^{(0)} = g_A \approx 1.27$  [6], as the difference formally contributes to higher chiral order. Existing lattice data indeed indicate that  $g_A$  has a mild  $m_\pi$  dependence [11,52]. The NLO LECs  $c_3$  and  $c_4$  have been extracted from pion-nucleon scattering [53,54]. They show a sizable dependence on the chiral order at which the fit to  $\pi$ - $N$  data is carried out, with a big change between NLO and N<sup>2</sup>LO, stabilizing between N<sup>2</sup>LO and N<sup>3</sup>LO. We find

$$\Delta_{A-V,\text{em}}^{(0)} \in \{2.4, 5.7\}, \quad \Delta_{A,\text{em}}^{(1)} = \{10.0, 14.5, 15.9\}, \quad (13)$$

where the range in  $\Delta_{A-V,\text{em}}^{(0)}$  is obtained by setting  $\hat{C}_A(\mu) - \hat{C}_V = 0$  and varying  $\mu$  between 0.5 and 1 GeV, while the three values of  $\Delta_{A,\text{em}}^{(1)}$  are obtained by using  $c_{3,4}$  extracted to NLO, N<sup>2</sup>LO, and N<sup>3</sup>LO [54]. While the NLO correction is somewhat larger than the leading-order (LO) one, we stress that we do not know the full LO correction because we have set the counterterm contribution  $\hat{C}_A - \hat{C}_V$  to zero. In addition, in an EFT without explicit  $\Delta$  degrees of freedom,  $c_3$  and  $c_4$  are dominated by  $\Delta$  contributions and thus

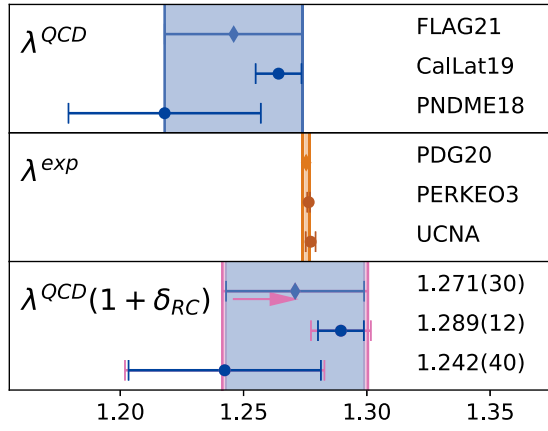


FIG. 2. Overview of the required shift to lattice QCD determinations of  $g_A$  and comparison with current experimental determination of  $\lambda$ . The bottom panel shows the shift and increased uncertainty in magenta with corrected values. The keys in the figure are FLAG21 [21], CalLat19 [22], PNDME18 [52], PDG20 [6], PERKEO3 [23], and UCNA [55].

anomalously large. Combining the corrections, we estimate a correction to  $\lambda$  at the percent level,

$$\delta_{RC}^{(\lambda)} \in \{1.4, 2.6\} \times 10^{-2}. \quad (14)$$

This large shift has no impact on the current first-row CKM discrepancy because the most accurate determination of  $\lambda$  is at present obtained from experiments, where these corrections are automatically included. On the other hand, the correction does have a big impact when comparing lattice QCD calculations of  $\lambda$ , currently performed in the isospin limit without QED, with the state-of-the-art experimental determinations of  $\lambda$ . We illustrate the significance of  $\delta_{RC}^{(\lambda)}$  in Fig. 2. Compared to the most precise individual lattice calculation [22], our radiative corrections corresponds to a  $2.7\sigma$  shift and a more modest  $\sim 1\sigma$  shift in the conservative FLAG'21 average [21].  $\delta_{RC}^{(\lambda)}$  generally improves the agreement between lattice QCD and experimental determination of  $\lambda$  and is essential if one wishes to obtain robust ranges (or constraints) on right-handed currents. For example, assuming existing central values and an increased lattice-QCD precision, the neglect of radiative corrections ( $\delta_{RC}^{(\lambda)}$ ) would wrongfully point to BSM physics at  $\mathcal{O}(1 \text{ TeV})$ .

The identified isospin-breaking corrections to weak magnetism in Eq. (8) do translate into explicit spectral changes. Compared to previous calculations we find significant shifts in  $a$ , the  $\beta$ - $\nu$  angular correlation, and  $A$ , the  $\beta$  asymmetry:

$$\begin{aligned} \frac{\delta \bar{a}}{\bar{a}} &= \frac{2\lambda \delta \mu_{\text{weak}}}{1 - \lambda^2} \frac{E_0 - 2E_e}{m_N}, \\ \frac{\delta \bar{A}}{\bar{A}} &= \frac{\delta \mu_{\text{weak}}}{2\lambda(1 - \lambda)} \left[ \frac{E_e - E_0}{m_N} + \frac{\lambda(E_0 - 3E_e)}{m_N} \right], \end{aligned} \quad (15)$$

where  $E_0$  is the maximum electron energy. These shift correspond to  $\mathcal{O}(10^{-4})$  corrections, which are comparable to anticipated experimental precision in the coming decade [12]. Even larger relative changes [ $\mathcal{O}(0.1\%)$ ] can occur due to cancellations in the leading-order SM prediction, such as in nuclear mirror systems used in complementary  $|V_{ud}|$  determinations [56]. An extension of this effort to nuclear systems is deemed crucial and fits within rejuvenated superallowed efforts [5,57]. The identified correction to the tensor coupling  $c_T$  in Eq. (9) produces additional shifts to the Fierz term and the neutrino-asymmetry parameter  $B$  at the level of  $10^{-5}$ . These are negligible in light of expected experimental accuracies

*Conclusions and outlook.*—By using a systematic effective field theory approach we have identified and computed novel radiative corrections to neutron  $\beta$  decay. The largest effect, at the percent level, is a QED correction to the nucleon axial charge. While this does not impact the extraction of  $V_{ud}$  from experiments, it has important consequences for the potential of  $\beta$  decay experiments to constrain BSM right-handed currents when comparing the measured value of  $\lambda = g_A/g_V$  to the first-principles calculation of the same quantity with lattice QCD. In addition, we have identified changes in the neutron differential decay rate, in particular a shift in the  $\beta$ - $\nu$  angular correlation and the  $\beta$  asymmetry, that can be measured in next-generation experiments.

The new shift in the nucleon axial charge depends on nonanalytic contributions associated with pion loops as well as analytic short-distance corrections parametrized by LECs. The LECs that lead to the largest part of the correction ( $c_3$  and  $c_4$ ) are precisely extracted from pion-nucleon scattering data, but others are presently unknown leading to a sizable uncertainty in our results. Lattice QCD can compute hadronic amplitudes in the presence of QED (for applications to meson decays see Refs. [19,20,58–60]), thus enabling a determination of the unknown LECs. QED<sub>M</sub> [61], in which the photon is given a nonzero mass, may simplify the lattice QCD determination by increasing the energy gap to the lowest excited state contamination, allowing an easier identification of the matrix element of interest.

Looking beyond neutron decay, it is very possible that similar-sized corrections affect nuclear  $\beta$  decay. The computations in this Letter provide the first step towards a full EFT treatment of radiative corrections to the multi-nucleon level, which is of great interest for precision tests of the standard model.

We thank Misha Gorchtein and Martin Hoferichter for interesting conversations. The work of A. W.-L. was supported in part by the U.S. Department of Energy, Office of Science, Office of Nuclear Physics under Awards No. DE-AC02-05CH11231. E. M. is supported by the U.S. Department of Energy through the Office of Nuclear Physics and the LDRD program at Los Alamos National

Laboratory. Los Alamos National Laboratory is operated by Triad National Security, LLC, for the National Nuclear Security Administration of U.S. Department of Energy (Contract No. 89233218CNA000001). J. d. V. acknowledges support from the Dutch Research Council (NWO) in the form of a VIDI grant. L. H. acknowledges support by the U.S. National Science Foundation (Grant No. PHY-1914133), U.S. Department of Energy (Grant No. DE-FG02-ER41042).

\*cirigliano@lanl.gov

†j.devries4@uva.nl

‡lmhayen@ncsu.edu

§emereghetti@lanl.gov

||walkloud@lbl.gov

- [1] C.-Y. Seng, M. Gorchtein, H. H. Patel, and M. J. Ramsey-Musolf, *Phys. Rev. Lett.* **121**, 241804 (2018).
- [2] C. Y. Seng, M. Gorchtein, and M. J. Ramsey-Musolf, *Phys. Rev. D* **100**, 013001 (2019).
- [3] A. Czarnecki, W. J. Marciano, and A. Sirlin, *Phys. Rev. D* **100**, 073008 (2019).
- [4] K. Shiells, P. G. Blunden, and W. Melnitchouk, *Phys. Rev. D* **104**, 033003 (2021).
- [5] J. C. Hardy and I. S. Towner, *Phys. Rev. C* **102**, 045501 (2020).
- [6] P. A. Zyla *et al.* (Particle Data Group), *Prog. Theor. Exp. Phys.* **2020**, 083C01 (2020).
- [7] A. Falkowski, M. González-Alonso, and O. Naviliat-Cuncic, *J. High Energy Phys.* **04** (2021) 126.
- [8] M. González-Alonso, O. Naviliat-Cuncic, and N. Severijns, *Prog. Part. Nucl. Phys.* **104**, 165 (2019).
- [9] T. Bhattacharya, V. Cirigliano, S. D. Cohen, A. Filipuzzi, M. Gonzalez-Alonso, M. L. Graesser, R. Gupta, and H.-W. Lin, *Phys. Rev. D* **85**, 054512 (2012).
- [10] S. Alioli, V. Cirigliano, W. Dekens, J. de Vries, and E. Mereghetti, *J. High Energy Phys.* **05** (2017) 086.
- [11] C. Chang *et al.*, *Nature (London)* **558**, 91 (2018).
- [12] V. Cirigliano, A. Garcia, D. Gazit, O. Naviliat-Cuncic, G. Savard, and A. Young, [arXiv:1907.02164](https://arxiv.org/abs/1907.02164).
- [13] D. Počanić *et al.*, *Nucl. Instrum. Methods Phys. Res., Sect. A* **611**, 211 (2009).
- [14] D. Dubbers, H. Abele, S. Baeßler, B. Märkisch, M. Schumann, T. Soldner, and O. Zimmer, *Nucl. Instrum. Methods Phys. Res., Sect. A* **596**, 238 (2008).
- [15] L. Hayen, *Phys. Rev. D* **103**, 113001 (2021).
- [16] M. Gorchtein and C.-Y. Seng, *J. High Energy Phys.* **10** (2021) 053.
- [17] A. Sirlin, *Phys. Rev.* **164**, 1767 (1967).
- [18] A. Sirlin, *Rev. Mod. Phys.* **50**, 573 (1978); **50**, 905(E) (1978).
- [19] N. Carrasco, V. Lubicz, G. Martinelli, C. T. Sachrajda, N. Tantalo, C. Tarantino, and M. Testa, *Phys. Rev. D* **91**, 074506 (2015).
- [20] D. Giusti, V. Lubicz, C. Tarantino, G. Martinelli, C. T. Sachrajda, F. Sanfilippo, S. Simula, N. Tantalo, and N. Tantalo, *Phys. Rev. Lett.* **120**, 072001 (2018).
- [21] Y. Aoki *et al.*, [arXiv:2111.09849](https://arxiv.org/abs/2111.09849).
- [22] A. Walker-Loud *et al.*, *Proc. Sci. CD2018* (2020) 020.
- [23] B. Märkisch, H. Mest, H. Saul, X. Wang, H. Abele, D. Dubbers, M. Klopff, A. Petoukhov, C. Roick, T. Soldner, and D. Werder, *Phys. Rev. Lett.* **122**, 242501 (2019).
- [24] J. Jackson, S. Treiman, and H. Wyld, *Phys. Rev.* **106**, 517 (1957).
- [25] S. Ando, H. W. Fearing, V. P. Gudkov, K. Kubodera, F. Myhrer, S. Nakamura, and T. Sato, *Phys. Lett. B* **595**, 250 (2004).
- [26] V. P. Gudkov, G. L. Greene, and J. R. Calarco, *Phys. Rev. C* **73**, 035501 (2006).
- [27] See Supplemental Material at <http://link.aps.org/supplemental/10.1103/PhysRevLett.129.121801> for definitions and detailed results, which includes Refs. [28–31].
- [28] S. R. Coleman, J. Wess, and B. Zumino, *Phys. Rev.* **177**, 2239 (1969).
- [29] C. G. Callan, Jr., S. R. Coleman, J. Wess, and B. Zumino, *Phys. Rev.* **177**, 2247 (1969).
- [30] V. Bernard, N. Kaiser, and U.-G. Meißner, *Int. J. Mod. Phys. E* **04**, 193 (1995).
- [31] S.-i. Ando, J. A. McGovern, and T. Sato, *Phys. Lett. B* **677**, 109 (2009).
- [32] A. Falkowski, M. González-Alonso, A. Palavrić, and A. Rodríguez-Sánchez, [arXiv:2112.07688](https://arxiv.org/abs/2112.07688).
- [33] J. Gasser and H. Leutwyler, *Ann. Phys. (N.Y.)* **158**, 142 (1984).
- [34] J. Gasser and H. Leutwyler, *Nucl. Phys.* **B250**, 465 (1985).
- [35] E. E. Jenkins and A. V. Manohar, *Phys. Lett. B* **255**, 558 (1991).
- [36] U.-G. Meißner and S. Steininger, *Phys. Lett. B* **419**, 403 (1998).
- [37] G. Müller and U.-G. Meißner, *Nucl. Phys.* **B556**, 265 (1999).
- [38] J. Gasser, M. A. Ivanov, E. Lipartia, M. Mojzis, and A. Rusetsky, *Eur. Phys. J. C* **26**, 13 (2002).
- [39] M. Knecht, H. Neufeld, H. Rupertsberger, and P. Talavera, *Eur. Phys. J. C* **12**, 469 (2000).
- [40] S. Weinberg, *Physica (Amsterdam)* **96A**, 327 (1979).
- [41] S. Weinberg, *Phys. Lett. B* **251**, 288 (1990).
- [42] S. Weinberg, *Nucl. Phys.* **B363**, 3 (1991).
- [43] R. E. Behrends and A. Sirlin, *Phys. Rev. Lett.* **4**, 186 (1960).
- [44] M. Ademollo and R. Gatto, *Phys. Rev. Lett.* **13**, 264 (1964).
- [45] J. F. Donoghue and D. Wyler, *Phys. Lett. B* **241**, 243 (1990).
- [46] V. Bernard, N. Kaiser, J. Kambor, and U.-G. Meißner, *Nucl. Phys.* **B388**, 315 (1992).
- [47] J. Kambor and M. Mojzis, *J. High Energy Phys.* **04** (1999) 031.
- [48] V. Bernard and U.-G. Meißner, *Phys. Lett. B* **639**, 278 (2006).
- [49] A. Sirlin, *Nucl. Phys.* **B196**, 83 (1982).
- [50] W. J. Marciano and A. Sirlin, *Phys. Rev. Lett.* **71**, 3629 (1993).
- [51] A. Czarnecki, W. J. Marciano, and A. Sirlin, *Phys. Rev. D* **70**, 093006 (2004).
- [52] R. Gupta, Y.-C. Jang, B. Yoon, H.-W. Lin, V. Cirigliano, and T. Bhattacharya, *Phys. Rev. D* **98**, 034503 (2018).

- [53] M. Hoferichter, J. Ruiz de Elvira, B. Kubis, and U.-G. Meißner, *Phys. Rep.* **625**, 1 (2016).
- [54] D. Siemens, J. Ruiz de Elvira, E. Epelbaum, M. Hoferichter, H. Krebs, B. Kubis, and U.-G. Meißner, *Phys. Lett. B* **770**, 27 (2017).
- [55] M. A. P. Brown *et al.* (UCNA Collaboration), *Phys. Rev. C* **97**, 035505 (2018).
- [56] O. Naviliat-Cuncic and N. Severijns, *Phys. Rev. Lett.* **102**, 142302 (2009).
- [57] M. Gorchtein, *Phys. Rev. Lett.* **123**, 042503 (2019).
- [58] M. Di Carlo, G. Martinelli, D. Giusti, V. Lubicz, C. T. Sachrajda, F. Sanfilippo, S. Simula, and N. Tantalo, *Proc. Sci., LATTICE2019* (2019) 196.
- [59] X. Feng, M. Gorchtein, L.-C. Jin, P.-X. Ma, and C.-Y. Seng, *Phys. Rev. Lett.* **124**, 192002 (2020).
- [60] P.-X. Ma, X. Feng, M. Gorchtein, L.-C. Jin, and C.-Y. Seng, *Phys. Rev. D* **103**, 114503 (2021).
- [61] M. G. Endres, A. Shindler, B. C. Tiburzi, and A. Walker-Loud, *Phys. Rev. Lett.* **117**, 072002 (2016).